ACS Macro Letters

Letter

Cite This: ACS Macro Lett. 2019, 8, 95−101

pubs.acs.org/macroletters

Glucose Single-Chain Polymer Nanoparticles for Cellular Targeting

A. Pia P. Kröger,[†] Muhabbat I. Komil,[†] Naomi M. Hamelmann,[†] Alberto Juan,[†,‡] Martina H. Stenzel,[§] and Jos M. J. Paulusse*[,†,∥]

[†]Department of Biomolecular Nanotechnology, MESA+ Institute for Nanotechnology and TechMed Institute for Health and Biomedical Technologies, Faculty of Science and Technology, University of Twente, P.O. Box 217, 7500 AE, Enschede, The Netherlands

[‡]Department of Molecular NanoFabrication, MESA+ Institute for Nanotechnology, Faculty of Science and Technology, University of Twente, P.O. Box 217, 7500 AE, Enschede, The Netherlands

[§]Centre for Advanced Macromolecular Design, School of Chemistry, The University of New South Wales, Sydney, NSW 2052, Australia

[∥]Department of Nuclear Medicine and Molecular Imaging, University Medical Center Groningen, P.O. Box 30.001, 9700 RB, Groningen, The Netherlands

Supporting Information

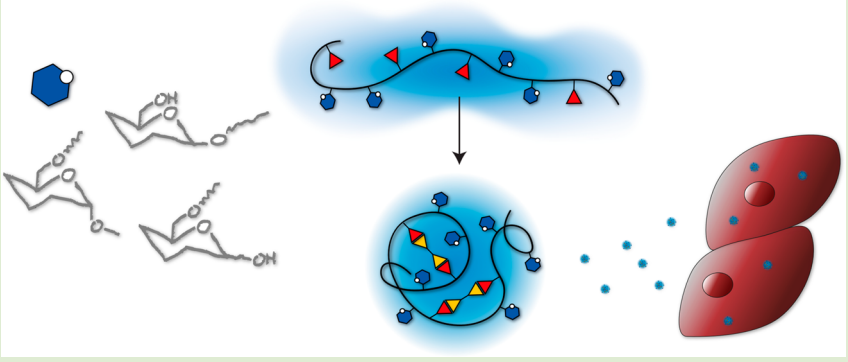

ABSTRACT: Naturally occurring glycoconjugates possess carbohydrate moieties that fulfill essential roles in many biological functions. Through conjugation of carbohydrates to therapeutics or imaging agents, naturally occurring glycoconjugates are mimicked and efficient targeting or increased cellular uptake of glycoconjugated macromolecules is achieved. In this work, linear and cyclic glucose moieties were functionalized with methacrylates via enzymatic synthesis and used as building blocks for intramolecular cross-linked single-chain glycopolymer nanoparticles (glyco-SCNPs). A set of water-soluble sub-10 nm-sized glyco-SCNPs was prepared by thiol-Michael addition cross-linking in water. Bioactivity of various glucose-conjugated glycopolymers and glyco-SCNPs was evaluated in binding studies with the glucose-specific lectin Concanavalin A and by comparing their cellular uptake efficiency in HeLa cells. Cytotoxicity studies did not reveal discernible cytotoxic effects, making these SCNPs promising candidates for ligand-based targeted imaging and drug delivery.

Biological functions of carbohydrates range widely from highly specific cellular recognition and communication, to the supply of energy.[1,2] Carbohydrate transport through the cell membrane is facilitated by specific membrane-bound carbohydrate transporters, that is, GLUT 1−14, which have therefore become popular targets for cell targeting with nanomaterials.[3,4] Furthermore, bacteria and viruses exhibit surfaces covered with carbohydrate-binding proteins, that is, lectins, with high binding affinity toward carbohydrates displayed on the targeted (human) cells.[5,6] This mimicry hinders recognition by the immune system and clearance of bacteria and viruses. Hence, functionalization of (polymer) nanomaterials with carbohydrates is a popular strategy to avoid immune response and furthermore may introduce targeting capabilities and increase cellular uptake.[4,7−12] For example, glucose-modified micelles were recently found to be taken up to an increased extent by cells with overexpressed GLUT 1 receptors and to cross the blood−brain barrier in fasting mice.[11] For successful brain uptake, glycaemic control of the mice diet and conjugation on the C6 position instead of the C3 position proved crucial, which suggests a transporter-mediated uptake mechanism. For the interaction between glucose and the transporter, mainly the C1−C3 hydroxyl groups are assumed to play a role.[13] Similarly, substitution of galactose either on C1 or C6 position was influential for the endocytic pathway of conjugated nanoparticles.[14]

Received: October 22, 2018
Accepted: November 26, 2018
Published: December 18, 2018

DOI: 10.1021/acsmacrolett.8b00812
ACS Macro Lett. 2019, 8, 95−101

To obtain glycopolymers and -nanoparticles, carbohydrate functionalities can either be attached postpolymerization or employed in the form of glycomonomers.[15−17] Controlled polymerization techniques, such as via reversible addition−fragmentation chain transfer (RAFT), offer superior structural control in both strategies. In case of postpolymerization functionalization, full substitution is impeded by steric hindrance and multistep protective group chemistry is typically required. Alternatively, glycomonomers are obtained via protective group chemistry or via enzymatic pathways providing chemo-, regio-, and stereoselectivity.[16−18]

The carbohydrate recognition efficacy of transporters depends on the architecture of the glycomacromolecule and varies with the carbohydrate hydroxyl group substitutions and carbohydrate linker density and spacing.[3,10,19,20] Not only in nature, but also synthetically, a variety of glycomacromolecule topologies is known, ranging from dendrimers to nanogels.[17,21−23] Multivalency in such structures is a striking factor to achieve selective binding toward the target site.[2,24,25] One way to evaluate the selective recognition of glycomacromolecules is to test their binding affinity to lectins. Concanavalin A (ConA) from *Canavalia ensiformis* (Jack bean) is one of the most studied lectins for modeling receptor interactions of glycomacromolecules, as it is structurally similar to a large number of bacterial and animal lectins in cell communication events.[25−27] Dendritic structures and micelles have shown superior binding as compared to linear polymer chains, as evaluated through ConA binding assays.[28−30] Whereas the complexity of the well-defined dendrimers increases with every generation, polymeric structures offer ease of synthesis, to certain extents at the cost of loss in structural control.

Single-chain polymer nanoparticles (SCNP) are prepared through exclusive intramolecular cross-linking of polymer chains and typically measure around 10 nm in diameter.[31−36] SCNPs are comparable in size to dendrimers, while the combination of polymer preparation techniques greatly alleviates synthetic effort. Recently, SCNPs have also been prepared from glycopolymers,[37−39] and current investigations are focused on controlling the structures of SCNPs and their biomedical applications.[40−44] Loinaz and co-workers have investigated SCNPs prepared from acrylate-functional dextran as a noninvasive drug delivery system targeted to the lungs, taking advantage of the small sizes of SCNPs. Further, Fulton and co-workers demonstrated that glyco-SCNPs from galactose or mannose conjugated polymers display specific molecular recognition by surfaces coated with ConA or with *E. coli* heat labile toxin.[38] Glyco-SCNPs prepared directly from polymerized acetylated-mannose monomers were developed by Barner-Kowollik and co-workers via cross-linking by UV irradiated tetrazole cycloaddition under ultrahigh dilution for subsequent cellular uptake experiments.[39] More recently, Becer and co-workers investigated lectin binding of SCNPs based on a cyclodextrin/adamantane-folded ABC triblock copolymer with a mannose acrylamide middle block.[45] Folding into SCNPs resulted in increased lectin binding in comparison to their linear precursors.

We previously demonstrated the drug encapsulation potential of water-soluble SCNPs, both in aqueous and organic medium.[46] Here, we report the development of analogous glucose-functional SCNPs and evaluation of their cell-targeting properties. Well-defined SCNPs were prepared, based on three different glucose-monomers, conjugated at the C1 or C6 glucose positions, and their in vitro cell targeting behavior was evaluated in relation to the mode of glucose functionalization. Precursor copolymers were prepared from enzymatically synthesized C1- and C6-functionalized glucose monomers and the corresponding SCNPs were subsequently obtained via thiol-Michael cross-linking of the precursor glycopolymers (Scheme 1). Bioactivities of the resulting SCNPs were compared based on their lectin binding abilities, reductive properties, cell toxicity, and uptake by HeLa cells.

Scheme 1. Schematic Representation of Glyco-SCNPs by Thiol-Michael Addition

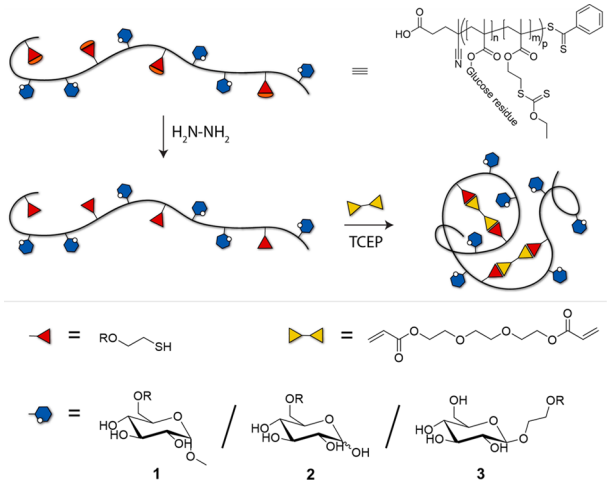

Glucose-based molecules were conjugated with methacrylate moieties via enzymatic coupling reactions based on literature procedures. Bead immobilized lipase from *Candida antarctica* catalyzed the conjugation at the C6 position as established by Davis and co-workers,[47] whereas β-glucosidase from almonds was used for C1 conjugation as described by the Loos group.[18] Conjugation at the C1 position blocks the opening of glucose to its linear form and due to the enzymatic reaction, only the β-anomer is formed **G_1MA** (**M3**), as confirmed by the absence of the H1-α signal in ^{1}H NMR spectroscopy. C6 conjugation was performed on methyl glucoside resulting in the formation of the **mG_6MA** monomer (**M1**), where the glucose is fixed in its α-ring pyranose form, as well as on glucose, resulting in the formation of the **G_6MA** monomer (**M2**), where the molecule can still interconvert between its open-chain form and the α/β anomers after conjugation. The thiol-functional monomer, xanthate methacrylate (**XMA**), was prepared following established literature procedures and combined via RAFT copolymerization with the glucose monomers.[48,49] Aliquots of the polymerizations were taken at regular intervals to confirm equal consumption of the monomers and hence to confirm a random copolymerization. Copolymers **P1**−**P3**, prepared from monomers **M1**−**M3**, were obtained with molecular weights of 40 kDa (**P1a**) and 100 kDa (**P1b**−**P3**) and with typical xanthate incorporation ratios of 15−20% (Table 1). Low dispersity indices (PDI) were achieved for the polymers ($Đ \sim$ 1.2), except for **P2** ($Đ$ = 1.5), as analyzed by gel permeation chromatography (GPC), which may suggest interaction between **M2** and the chain transfer agent (CTA).

SCNP formation from glucose-containing precursor polymers was based on a protocol that we developed previously for glycerol-xanthate copolymers.[46] After deprotection of the xanthate moiety with hydrazine, as observed with ^{1}H NMR spectroscopy (Figure S3), the obtained thiol polymers were

DOI: 10.1021/acsmacrolett.8b00812
ACS Macro Lett. 2019, 8, 95−101

Table 1. Comparison of Molecular Weights of Glycopolymers and Their Corresponding Nanoparticles

	$M_{n,theo}$[a] (kg/mol)	$M_{n,GPC}$[b] (kg/mol)	$M_{n,MALS}$[c] (kg/mol)	χ_{SH}	$Đ$[b]	ΔM_{app}[e] (%)	$r_{H,DLS}$[f] (nm)	$r_{H,DOSY}$[f] (nm)	$r_{H,visco}$[d] (nm)	$[\eta]$[d] (mL/g)
P1a	40	32		14	1.13		3.4	3.9		
Np1a		22			1.16	30	3.4	3.7		
P1b	108	154	102	17	1.31		6.4		9.4	33.4
Np1[b]		101	91		1.13	34	2.8		8.0	26.8
P2	105	89	70	15	1.45		5.9		7.8	23.6
NP2		63	87		1.46	30	3.2		12.4	28.1
P3	102	105	83	20	1.23		5.7		8.8	27.2
NP3		80	65		1.10	24	1.9		6.2	19.4

[a]Determined by ^{1}H NMR. [b]Determined in DMF by GPC, relative to PEG standards. [c]Determined in DMF by GPC, by MALS measurements. [d]Determined in DMF by GPC, by a viscometer. [e]Reduction in apparent number-average molecular weight, calculated as $\Delta M_{app} = -((M_{n,NP} - M_{n,P})/M_{n,NP}) \times 100\%$. [f]Measured in H_2O/D_2O.

slowly added to a carbonate buffered solution containing PEG diacrylate and tris(2-carboxyethyl)phosphine. Dimethylaminoethyl acrylate was added toward the end of the reaction to functionalize any remaining unreacted thiols. ^{1}H NMR measurements confirmed successful thiol-Michael addition by additional signals between 2.8 and 3.0 ppm (Figures S4–S7).

To observe the chain collapse caused by intramolecular cross-linking, GPC measurements were performed, which revealed an apparent size reduction of around 30% (Table 1 and Figure 1). Moreover, multiangle light scattering (MALS) confirmed constant molecular weights for **NP1b** and **NP3**, as compared to their precursor polymers **P1b** and **P3** (Figure S9).

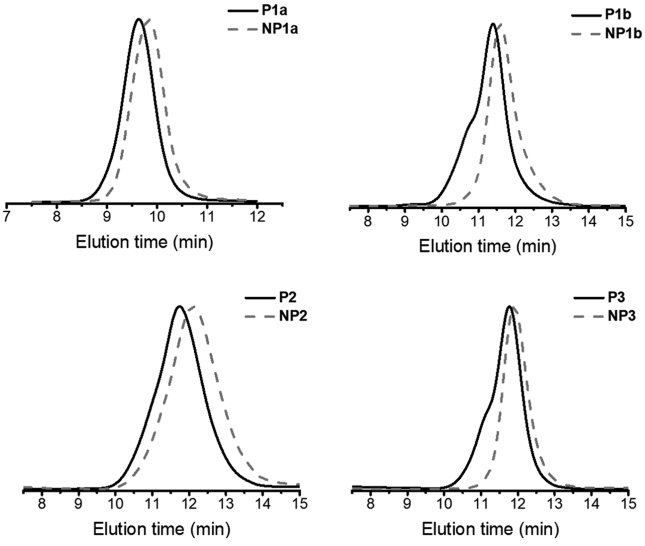

Figure 1. Overlay of GPC traces for the glycocopolymer precursors (**P1–3**) with different chain lengths and their corresponding nanoparticles (**NP1–3**).

Furthermore, intrinsic viscosities $[\eta]$ were reduced after cross-linking, which is related to a reduced hydrodynamic radius and hence to intramolecular cross-linking. Plotting differential weight fraction against molar mass does not indicate increases in molar mass upon cross-linking, therefore excluding multichain-aggregates and thus pointing to exclusive intramolecular cross-linking. However, **NP2** displayed an increased M_n, indicating formation of intermolecular cross-links. Differential molar mass weight fractions of **NP2** confirmed the coexistence of multichain aggregates of **NP2** with higher M_n than the original polymer. The formation of multichain aggregates precludes a reduction of $[\eta]$, but the differential intrinsic viscosity weight fraction does reveal presence majority of fractions with reduced $[\eta]$. Despite the presence of intermolecular cross-links (<20%, Figure S9), intramolecular cross-linking is predominant.

For polymers **P1a**, **P2**, and **P3** ($M_n \geq 90$ kDa), size reductions were observed in dynamic light scattering (DLS) upon SCNP formation (Table 1 and Figure S8). In the case of the shortest precursor polymer (**P1b**, 40 kDa), a reduction in size was not detectable with DLS. However, additional measurements with diffusion-ordered spectroscopy (DOSY) NMR on **P1a** and **NP1a** revealed a slight particle size reduction from 3.9 to 3.7 nm. Furthermore, transmission electron microscopy (TEM) on negatively stained **NP1a** revealed particles of around 5 nm in radius with a uniform particle shape and size (Figure S10).

The reducing characteristics of the glucose monomeric units in the prepared polymers and SCNPs were evaluated with Benedict's reagent (Figure 2), a citrate solution that complexates copper(II), resulting in a blue color.[50] Formation of red copper precipitates in Benedict's solution with **P2** and **NP2** confirms preservation of reducing properties of the glucose monomeric units. Hence, ring-opening of glucose in **M2** is not blocked by polymerization or cross-linking. For the other polymers and nanoparticles, no color change was expected as the glucosides are present in the pyranose, nonreducing form. Surprisingly, polymers **P1** and **P3** result in green colors when performing the reduction assay, while the **NP1** and **NP3** solutions stayed blue as the negative control. Diethyldithiocarbamates, comparable to the CTA- and xanthate moieties on polymers **P1** and **P3**, have been reported earlier to form copper complexes with $CuCl_2$, resulting in color changes from green to brown.[51] As controls, the RAFT homopolymers pHEMA and a glycerol methacrylate-*co*-**XMA** copolymer were tested with Benedict's reagent. Whereas pHEMA did not result

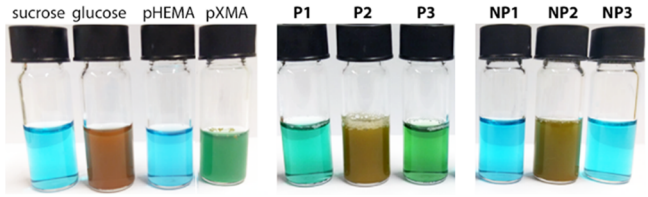

Figure 2. Bendicts assay with glycopolymers (**P1–3**) and corresponding nanoparticles (**NP1–3**) (sucrose = negative control, glucose = positive control, pHEMA = polymer with same CTA, pXMA = copolymer containing XMA).

DOI: 10.1021/acsmacrolett.8b00812
ACS Macro Lett. 2019, 8, 95–101

in a color change, the **XMA** copolymer revealed a similar color shift as polymers **P1** and **P3**. Presumably, the color change is therefore due to copper interactions with the xanthate moieties and is not caused by the glucose functionalities. Neither monomer synthesis, nor polymerization or SCNP formation, affected the nonreducing and reducing properties of the glucoside and glucose monomeric units, respectively.

ConA is a lectin with four binding sites at pH 7, which are specifically sensitive to glucose moieties.[25,27] Various carbohydrate conjugated positional isomers have been thoroughly investigated, demonstrating specificity of ConA toward α-glucose over β-glucose, while substitution of hydroxyl groups at the 3-, 4-, and 6-carbon positions has shown to disrupt carbohydrate recognition.[52] Therefore, the binding ability of C1- and C6-functionalized glucose repeating units in polymers **P1**−**P3** and nanoparticles **NP1**−**NP3** was tested in a quantitative ConA precipitation assay. In agreement with literature reports, polymers with glycomonomers functionalized at the C6 position (**P1** and **P2**), and the corresponding SCNPs (**NP1** and **NP2**) showed a lower binding affinity toward ConA.[52] Interestingly, ConA did not even precipitate when exposed to **P2** or **NP2** and precipitation was inhibited, comparable to monomeric glucose. In contrast, **P3** and **NP3** with C1-functionalized glucose in its β-configuration were indeed recognized by ConA, where **NP3** displayed a significantly decreased binding affinity toward ConA as compared to its linear precursor **P3** (Figure S11). **P3**/**NP3** not only contain a C1-conjugated glucose, but also a longer linker (one methylene unit) between glucose moiety and acrylate group than in the case of **P1**/**NP1** and **P2**/**NP2**, which might enhance ConA recognition. Since the SCNP is no longer linear, but rather collapsed and cross-linked, the glucose moieties are likely less available for formation of clusters with lectins. The decreased lectin binding upon SCNP formation is in contrast with the findings of Becer and co-workers with C-shaped mannose SCNPs, where the mannose units are incorporated in the middle segment of the polymer, and only the end blocks are cross-linked.[45] The difference between the studies highlights the importance of the secondary structure of glycomacromolecules on molecular recognition. Here, the ConA binding studies confirm the positional dependency of glucose functionalization on molecular recognition and point toward reduced flexibility of the polymer chain after cross-linking. However, interaction of glycomacromolecules with a single lectin is not representative for the wide range of interactions between cell receptors, proteins, and transporters. In order to further evaluate the effects of the positional isomers of glycoconjugates, in vitro studies were performed with each conjugate.

HeLa cells express predominantly GLUT1 and GLUT3 as glucose transporters and were therefore selected for our investigations.[53] Cytotoxicity of the different SCNPs was evaluated at concentrations up to 200 μg/mL. None of the polymers or SCNPs displayed significant toxicity, even at the highest concentrations, after 24 or 48 h and likewise no concentration dependency could be discerned (Figure S12). Additional evaluation of **P1** and **NP1** on human endothelial brain cells (hCMEC/D3) also did not reveal notable effects on cell viability.

In order to facilitate cell uptake studies, particles were fluorescently labeled with 5-(4,6-dichlorotriazinyl)-aminofluorescein (DTAF), which was confirmed by GPC equipped with fluorescence detector. As free label was still detectable after extensive dialysis, the samples were purified by FPLC prior to cell experiments. **NP1**−**3** were incubated with HeLa cells and FACS experiments were conducted at different incubation time points to quantify nanoparticle uptake (Figure 3). For all nanoparticles, cellular uptake was confirmed and

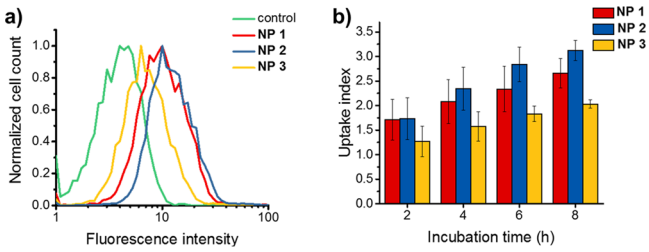

Figure 3. FACS analysis of uptake of glyco-SCNP (**NP1**−**3**) to HeLa cells: (a) Histogram after 8 h of incubation; (b) Uptake index (UI) over time (UI = mean fluorescence intensity (MFI) of treated cells/MFI of control cells).

increased with incubation time. Highest uptake was observed for **NP2**, comprising glucose with a free C1 position. Lowest uptake was clearly observed for **NP3**, with glucose moieties conjugated at the C1 position. **NP1**, which is composed of C6-conjugated glucose with a modified C1 position, is taken up to an intermediate amount.

To further investigate the uptake mechanism, the nanoparticle uptake to HeLa cells was studied in combination with confocal microscopy. In agreement with the FACS results, all three nanoparticles **NP1**−**3** were observed inside of the cells, while the fluorescence intensity is substantially reduced in the case of **NP3**. As the confocal images show clear vesiculation of the nanoparticles, early endosomes, late endosomes, and lysosomes were stained in addition to the nucleus and membrane (Figures 4 and S14−17). After 4 h of incubation, fluorescence of the SCNPs only partially overlapped with early endosomes, but strong colocalization with the late endosome and lysosome staining was observed for all nanoparticles. Furthermore, the intensity of the endosome and lysosome staining is strongly increased in the case of **NP1** and **NP2** incubation in contrast to the control cells.

In combination with the differing cellular uptake for the three glyco-SCNPs, these results strongly suggest receptor-mediated uptake to the HeLa cells. For cellular recognition, the C1 position of the glucose hydroxyl groups is more relevant than the C6 position. However, methylation of the C1 hydroxyl does not impede uptake drastically, which supports that not one single hydroxyl group is solely responsible for recognition.[11,13] Further, the similar cellular uptake behavior of **NP1** and **NP2** also implies that the linear structure of glucose is not essential for recognition and that the pyranose form participates in receptor binding.

In this work, we describe the synthesis and incorporation of C1- and C6-glucose-derived methacrylates into RAFT copolymers and into SCNPs. Furthermore, the resulting nanoparticles were compared with regards to molecular recognition and targeting behavior. The reductive properties of the C6-glucose moiety were preserved upon RAFT copolymerization, as well as cross-linking via thiol-Michael addition and are, hence, expected to be also accessible in cellular environments. Evaluation of the glyco-SCNPs in ConA binding assays revealed strongest binding when the C6 position of glucose remains accessible. While all three glyco-

DOI: 10.1021/acsmacrolett.8b00812
ACS Macro Lett. 2019, 8, 95−101

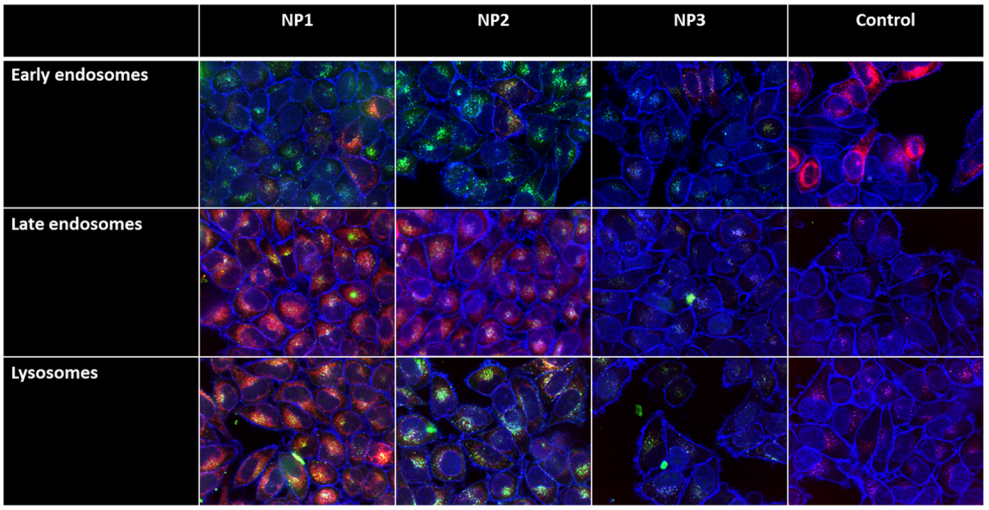

Figure 4. Overlaid confocal images of HeLa cells incubated 4 h with the glyco-SCNPs **NP1−3** (in green, nuclei and membrane = blue, cell compartment = red).

SCNPs were taken up via the endocytic pathway, the efficiency of their uptake to HeLa cells differed. Comparison of the cellular uptake efficiency of SCNPs with glucose moieties conjugated through the C1 and C6 position, in their blocked pyranose and in their partly linear form, demonstrates that the effect of a reducing glucose is minor in comparison to the position of conjugation. Accordingly, equipping SCNPs with glycoligands provides control over cell targeting, which may be exploited in tumor targeting.

■ ASSOCIATED CONTENT

Supporting Information

The Supporting Information is available free of charge on the ACS Publications website at DOI: 10.1021/acsmacrolett.8b00812.

Experimental details, polymerization plots, ^{1}H NMR spectra, DLS/GPC data, TEM image, cytotoxicity/lectin binding studies, and confocal images (PDF).

■ AUTHOR INFORMATION

Corresponding Author

*E-mail: j.m.j.paulusse@utwente.nl.

ORCID

A. Pia P. Kröger: 0000-0001-7031-0598
Naomi M. Hamelmann: 0000-0002-7126-4818
Alberto Juan: 0000-0002-4159-9772
Martina H. Stenzel: 0000-0002-6433-4419
Jos M. J. Paulusse: 0000-0003-0697-7202

Author Contributions

All authors have given approval to the final version of the manuscript.

Notes

The authors declare no competing financial interest.

■ ACKNOWLEDGMENTS

The Netherlands Organization for Health Research and Development (ZonMw, Project Number 733050304) and Alzheimer Nederland are thanked for funding. Funding from the EuroNanoMed III research program (Ref. EURONANOMED2017-178) is gratefully acknowledged. We thank Maaike Schotman and Regine van der Hee for support in cell experiments. We thank Prof. Dr. Julius Vancso and Dr. Maciej Kopeć for fruitful discussions and collaborations. Furthermore, the team of Wyatt Technology Europe GmbH for MALS analysis and Dr. E. G. Keim is thanked for TEM measurements.

■ REFERENCES

(1) Ladmiral, V.; Melia, E.; Haddleton, D. M. Synthetic Glycopolymers: An Overview. *Eur. Polym. J.* **2004**, *40* (3), 431−449.
(2) Kiessling, L. L.; Grim, J. C. Glycopolymer Probes of Signal Transduction. *Chem. Soc. Rev.* **2013**, *42* (10), 4476−4491.
(3) Patra, M.; Awuah, S. G.; Lippard, S. J. Chemical Approach to Positional Isomers of Glucose−Platinum Conjugates Reveals Specific Cancer Targeting through Glucose-Transporter-Mediated Uptake *in Vitro* and *in Vivo*. *J. Am. Chem. Soc.* **2016**, *138* (38), 12541−12551.
(4) Zhao, J.; Babiuch, K.; Lu, H.; Dag, A.; Gottschaldt, M.; Stenzel, M. H. Fructose-Coated Nanoparticles: A Promising Drug Nanocarrier for Triple-Negative Breast Cancer Therapy. *Chem. Commun.* **2014**, *50* (100), 15928−15931.
(5) Wesener, D. A.; Wangkanont, K.; McBride, R.; Song, X.; Kraft, M. B.; Hodges, H. L.; Zarling, L. C.; Splain, R. A.; Smith, D. F.; Cummings, R. D.; Paulson, J. C.; Forest, K. T.; Kiessling, L. L. Recognition of Microbial Glycans by Human Intelectin-1. *Nat. Struct. Mol. Biol.* **2015**, *22* (8), 603−610.
(6) Raman, R.; Tharakaraman, K.; Sasisekharan, V.; Sasisekharan, R. Glycan-Protein Interactions in Viral Pathogenesis. *Curr. Opin. Struct. Biol.* **2016**, *40*, 153−162.
(7) Dag, A.; Callari, M.; Lu, H.; Stenzel, M. H. Modulating the Cellular Uptake of Platinum Drugs with Glycopolymers. *Polym. Chem.* **2016**, *7* (5), 1031−1036.
(8) Li, J.; Ma, F.-K.; Dang, Q.-F.; Liang, X.-G.; Chen, X.-G. Glucose-Conjugated Chitosan Nanoparticles for Targeted Drug Delivery and Their Specific Interaction with Tumor Cells. *Front. Mater. Sci.* **2014**, *8* (4), 363−372.
(9) Gromnicova, R.; Davies, H. A.; Sreekanthreddy, P.; Romero, I. A.; Lund, T.; Roitt, I. M.; Phillips, J. B.; Male, D. K. Glucose-Coated Gold Nanoparticles Transfer across Human Brain Endothelium and Enter Astrocytes In Vitro. *PLoS One* **2013**, *8* (12), No. e81043.
(10) Xie, F.; Yao, N.; Qin, Y.; Zhang, Q.; Chen, H.; Yuan, M.; Tang, J.; Li, X.; Fan, W.; Zhang, Q.; Wu, Y.; Hai, L.; He, Q. Investigation of Glucose-Modified Liposomes Using Polyethylene Glycols with Different Chain Lengths as the Linkers for Brain Targeting. *Int. J. Nanomed.* **2012**, *7*, 163−175.

DOI: 10.1021/acsmacrolett.8b00812
ACS Macro Lett. 2019, 8, 95−101

(11) Anraku, Y.; Kuwahara, H.; Fukusato, Y.; Mizoguchi, A.; Ishii, T.; Nitta, K.; Matsumoto, Y.; Toh, K.; Miyata, K.; Uchida, S.; Nishina, K.; Osada, K.; Itaka, K.; Nishiyama, N.; Mizusawa, H.; Yamasoba, T.; Yokota, T.; Kataoka, K. Glycaemic Control Boosts Glucosylated Nanocarrier Crossing the BBB into the Brain. *Nat. Commun.* **2017**, *8* (1), 1001−1010.
(12) Seidi, F.; Jenjob, R.; Phakkeeree, T.; Crespy, D. Saccharides, Oligosaccharides, and Polysaccharides Nanoparticles for Biomedical Applications. *J. Controlled Release* **2018**, *284*, 188−212.
(13) Barnett, J. E.; Holman, G. D.; Munday, K. A. Structural Requirements for Binding to the Sugar-Transport System of the Human Erythrocyte. *Biochem. J.* **1973**, *131* (2), 211−221.
(14) Sun, P.; He, Y.; Lin, M.; Zhao, Y.; Ding, Y.; Chen, G.; Jiang, M. Glyco-Regioisomerism Effect on Lectin-Binding and Cell-Uptake Pathway of Glycopolymer-Containing Nanoparticles. *ACS Macro Lett.* **2014**, *3* (1), 96−101.
(15) Narain, R.; Armes, S. P. Synthesis and Aqueous Solution Properties of Novel Sugar Methacrylate-Based Homopolymers and Block Copolymers. *Biomacromolecules* **2003**, *4* (6), 1746−1758.
(16) Albertin, L.; Kohlert, C.; Stenzel, M. H.; Foster, J. R.; Davis, T. P. Chemoenzymatic Synthesis of Narrow-Polydispersity Glycopolymers: Poly(6-O-Vinyladipolyl-D-Glucopyranose). *Biomacromolecules* **2004**, *5* (2), 255−260.
(17) Becer, C. R. The Glycopolymer Code: Synthesis of Glycopolymers and Multivalent Carbohydrate-Lectin Interactions. *Macromol. Rapid Commun.* **2012**, *33* (9), 742−752.
(18) Kloosterman, W. M. J.; Roest, S.; Priatna, S. R.; Stavila, E.; Loos, K. Chemo-Enzymatic Synthesis Route to Poly(Glucosyl-Acrylates) Using Glucosidase from Almonds. *Green Chem.* **2014**, *16* (4), 1837−1846.
(19) Kiessling, L. L.; Kraft, M. B. Chemistry. A Path to Complex Carbohydrates. *Science (Washington, DC, U. S.)* **2013**, *341* (6144), 357−358.
(20) Polizzotti, B. D.; Maheshwari, R.; Vinkenborg, J.; Kiick, K. L. Effects of Saccharide Spacing and Chain Extension on Toxin Inhibition by Glycopolypeptides of Well-Defined Architecture. *Macromolecules* **2007**, *40* (20), 7103−7110.
(21) Turnbull, W. B.; Stoddart, J. F. Design and Synthesis of Glycodendrimers. *Rev. Mol. Biotechnol.* **2002**, *90* (3−4), 231−255.
(22) Abdouni, Y.; Yilmaz, G.; Becer, C. R. Sequence and Architectural Control in Glycopolymer Synthesis. *Macromol. Rapid Commun.* **2017**, *38* (24), 1700212.
(23) Bernard, J.; Hao, X.; Davis, T. P.; Barner-Kowollik, C.; Stenzel, M. H. Synthesis of Various Glycopolymer Architectures via RAFT Polymerization: From Block Copolymers to Stars. *Biomacromolecules* **2006**, *7* (1), 232−238.
(24) Pohl, N. L.; Kiessling, L. L. Scope of Multivalent Ligand Function. Lactose-Bearing Neoglycopolymers by Ring-Opening Metathesis Polymerization. *Synthesis* **1999**, *1999* (S1), 1515−1519.
(25) Cairo, C. W.; Gestwicki, J. E.; Kanai, M.; Kiessling, L. L. Control of Multivalent Interactions by Binding Epitope Density. *J. Am. Chem. Soc.* **2002**, *124* (8), 1615−1619.
(26) Kobayashi, K.; Sumitomo, H.; Ina, Y. Synthesis and Functions of Polystyrene Derivatives Having Pendant Oligosaccharides. *Polym. J.* **1985**, *17* (4), 567−575.
(27) Goldstein, I. J.; Hayes, C. E. The Lectins: Carbohydrate-Binding Proteins of Plants and Animals. *Adv. Carbohydr. Chem. Biochem.* **1978**, *35* (C), 127−340.
(28) Hetzer, M.; Chen, G.; Barner-Kowollik, C.; Stenzel, M. H. Neoglycopolymers Based on 4-Vinyl-1,2,3-Triazole Monomers Prepared by Click Chemistry. *Macromol. Biosci.* **2010**, *10* (2), 119−126.
(29) Kumar, J.; Bousquet, A.; Stenzel, M. H. Thiol-Alkyne Chemistry for the Preparation of Micelles with Glycopolymer Corona: Dendritic Surfaces versus Linear Glycopolymer in Their Ability to Bind to Lectins. *Macromol. Rapid Commun.* **2011**, *32* (20), 1620−1626.
(30) Martin, A. L.; Li, B.; Gillies, E. R. Surface Functionalization of Nanomaterials with Dendritic Groups: Toward Enhanced Binding to Biological Targets. *J. Am. Chem. Soc.* **2009**, *131* (2), 734−741.
(31) Aiertza, M. K.; Odriozola, I.; Cabañero, G.; Grande, H.-J.; Loinaz, I. Single-Chain Polymer Nanoparticles. *Cell. Mol. Life Sci.* **2012**, *69* (3), 337−346.
(32) Lyon, C. K.; Prasher, A.; Hanlon, A. M.; Tuten, B. T.; Tooley, C. A.; Frank, P. G.; Berda, E. B. A Brief User's Guide to Single-Chain Nanoparticles. *Polym. Chem.* **2015**, *6* (2), 181−197.
(33) González-Burgos, M.; Latorre-Sánchez, A.; Pomposo, J. A. Advances in Single Chain Technology. *Chem. Soc. Rev.* **2015**, *44* (17), 6122−6142.
(34) Altintas, O.; Barner-Kowollik, C. Single-Chain Folding of Synthetic Polymers: A Critical Update. *Macromol. Rapid Commun.* **2016**, *37* (1), 29−46.
(35) Mavila, S.; Eivgi, O.; Berkovich, I.; Lemcoff, N. G. Intramolecular Cross-Linking Methodologies for the Synthesis of Polymer Nanoparticles. *Chem. Rev.* **2016**, *116* (3), 878−961.
(36) Pomposo, J. A. Single-Chain Polymer Nanoparticles: Synthesis, Characterization, Simulations, and Applications; Wiley, 2017.
(37) Gracia, R.; Marradi, M.; Cossío, U.; Benito, A.; Pérez-San Vicente, A.; Gómez-Vallejo, V.; Grande, H.-J.; Llop, J.; Loinaz, I. Synthesis and Functionalization of Dextran-Based Single-Chain Nanoparticles in Aqueous Media. *J. Mater. Chem. B* **2017**, *5* (6), 1143−1147.
(38) Mahon, C. S.; McGurk, C. J.; Watson, S. M. D.; Fascione, M. A.; Sakonsinsiri, C.; Turnbull, W. B.; Fulton, D. A. Molecular Recognition-Mediated Transformation of Single-Chain Polymer Nanoparticles into Crosslinked Polymer Films. *Angew. Chem., Int. Ed.* **2017**, *56* (42), 12913−12918.
(39) Wuest, K. N. R.; Lu, H.; Thomas, D. S.; Goldmann, A. S.; Stenzel, M. H.; Barner-Kowollik, C. Fluorescent Glyco Single-Chain Nanoparticle-Decorated Nanodiamonds. *ACS Macro Lett.* **2017**, *6* (10), 1168−1174.
(40) Zhang, J.; Gody, G.; Hartlieb, M.; Catrouillet, S.; Moffat, J.; Perrier, S. Synthesis of Sequence-Controlled Multiblock Single Chain Nanoparticles by a Stepwise Folding−Chain Extension−Folding Process. *Macromolecules* **2016**, *49* (23), 8933−8942.
(41) Mes, T.; van der Weegen, R.; Palmans, A. R. A.; Meijer, E. W. Single-Chain Polymeric Nanoparticles by Stepwise Folding. *Angew. Chem., Int. Ed.* **2011**, *50* (22), 5085−5089.
(42) Huo, M.; Wang, N.; Fang, T.; Sun, M.; Wei, Y.; Yuan, J. Single-Chain Polymer Nanoparticles: Mimic the Proteins. *Polymer* **2015**, *66*, A11−A21.
(43) Cole, J. P.; Lessard, J. J.; Rodriguez, K. J.; Hanlon, A. M.; Reville, E. K.; Mancinelli, J. P.; Berda, E. B. Single-Chain Nanoparticles Containing Sequence-Defined Segments: Using Primary Structure Control to Promote Secondary and Tertiary Structures in Synthetic Protein Mimics. *Polym. Chem.* **2017**, *8* (38), 5829−5835.
(44) Kröger, A. P. P.; Paulusse, J. M. J. Single-Chain Polymer Nanoparticles in Controlled Drug Delivery and Targeted Imaging. *J. Controlled Release* **2018**, *286*, 326−347.
(45) Yilmaz, G.; Uzunova, V.; Napier, R.; Becer, C. R. Single-Chain Glycopolymer Folding via Host−Guest Interactions and Its Unprecedented Effect on DC-SIGN Binding. *Biomacromolecules* **2018**, *19*, 3040.
(46) Kröger, A. P. P.; Hamelmann, N. M.; Juan, A.; Lindhoud, S.; Paulusse, J. M. J. Biocompatible Single-Chain Polymer Nanoparticles for Drug Delivery − a Dual Approach. *ACS Appl. Mater. Interfaces* **2018**, *10*, 30946.
(47) Albertin, L.; Stenzel, M. H.; Barner-Kowollik, C.; Foster, L. J. R.; Davis, T. P. Well-Defined Glycopolymers from RAFT Polymerization: Poly(Methyl 6-O-Methacryloyl-R-D -Glucoside) and Its Block Copolymer with 2-Hydroxyethyl Methacrylate. *Macromolecules* **2004**, *37*, 7530−7537.
(48) Nicolaÿ, R. Synthesis of Well-Defined Polythiol Copolymers by RAFT Polymerization. *Macromolecules* **2012**, *45* (2), 821−827.

DOI: 10.1021/acsmacrolett.8b00812
ACS Macro Lett. 2019, 8, 95−101

(49) Kröger, A. P. P.; Boonen, R. J. E. A.; Paulusse, J. M. J. Well-Defined Single-Chain Polymer Nanoparticles via Thiol-Michael Addition. *Polymer* **2017**, *120*, 119−128.
(50) Benedict, S. R. A. Reagent for the Detection of Reducing Sugars. *J. Biol. Chem.* **1908**, *5*, 485−487.
(51) Pang, H.; Chen, D.; Cui, Q.; Dou, Q. Sodium Diethyldithiocarbamate, an AIDS Progression Inhibitor and a Copper-Binding Compound, Has Proteasome-Inhibitory and Apoptosis-Inducing Activities in Cancer Cells. *Int. J. Mol. Med.* **2007**, *19* (5), 809−816.
(52) Goldstein, I. J.; Hollerman, C. E.; Smith, E. E. Protein-Carbohydrate Interaction. II. Inhibition Studies on the Interaction of Concanavalin A with Polysaccharides. *Biochemistry* **1965**, *4* (5), 876−883.
(53) Rodríguez-Enríquez, S.; Marín-Hernández, A.; Gallardo-Pérez, J. C.; Moreno-Sánchez, R. Kinetics of Transport and Phosphorylation of Glucose in Cancer Cells. *J. Cell. Physiol.* **2009**, *221* (3), 552−559.

DOI: 10.1021/acsmacrolett.8b00812
ACS Macro Lett. 2019, 8, 95−101